Supplementary Materials

Ni(II) Complexes of 2-Imine-8-Hydroxyquinolines: Characterization, Albumin Binding and Cytotoxicity

Sofia Marcão [1,†], Leonor Côrte-Real [1,†], Alice Alborghetti [1], Maël Dejoux [1], Gabriella Spengler [2], Xavier Fontrodona [3], Isabel Romero [3], Éva A. Enyedy [4], Alexandra M. M. Antunes [1] and Isabel Correia [1,*]

[1] Centro de Química Estrutural and Departamento de Engenharia Química, Institute of Molecular Sciences, Instituto Superior Técnico, Universidade de Lisboa, Av. Rovisco Pais 1, 1049-001 Lisboa, Portugal; sofiadvmarcao@tecnico.ulisboa.pt (S.M.); leonor.corte-real@tecnico.ulisboa.pt (L.C.-R.); alice.alborghetti97@gmail.com (A.A.); maeldjx01@gmail.com (M.D.); alexandra.antunes@tecnico.ulisboa.pt (A.M.M.A.)

[2] Department of Medical Microbiology, Albert Szent-Györgyi Health Center and Albert Szent-Györgyi Medical School, University of Szeged, Semmelweis u. 6, H-6725 Szeged, Hungary; spengler.gabriella@med.u-szeged.hu

[3] Departament de Química i Serveis Tècnics de Recerca, Universitat de Girona, C/M Aurèlia Capmany, 69, E-17003 Girona, Spain; xavier.fontrodona@udg.edu (X.F.); marisa.romero@udg.edu (I.R.)

[4] Department of Molecular and Analytical Chemistry, University of Szeged, Dóm tér 7-8., H-6720 Szeged, Hungary; enyedy@chem.u-szeged.hu

* Correspondence: icorreia@tecnico.ulisboa.pt

† These authors contributed equally to this work.

S1 – FTIR SPECTRA 2

S2 – ESI-MS DATA 5

S3 – UV-VIS MOLECULAR SPECTRA 9

S4 – SCXRD CHARACTERIZATION 11

S5 – SOLUTION STABILITY 14

S6 – BSA BINDING 18

S1 – FTIR spectra

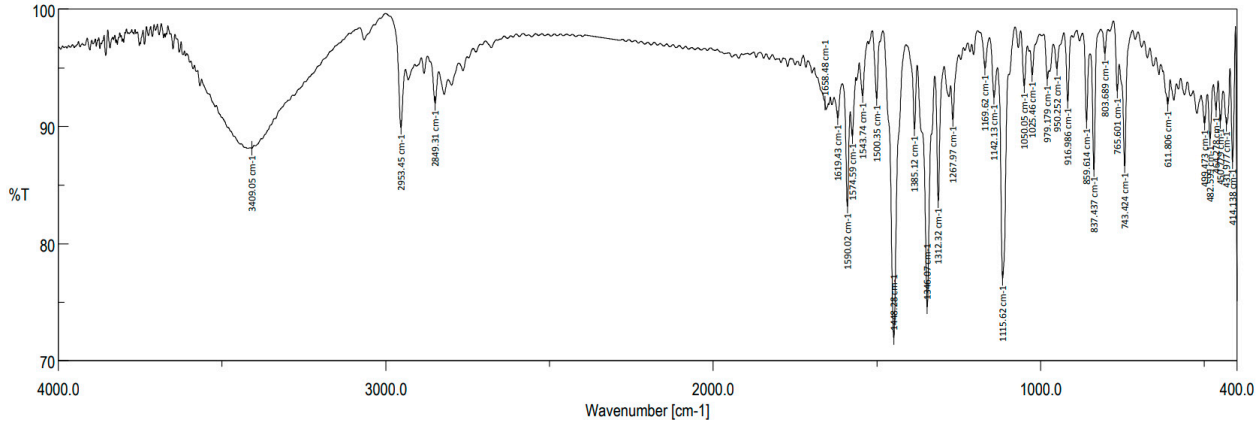


Fig. S1. FTIR spectrum of complex **1** measured in KBr disks.

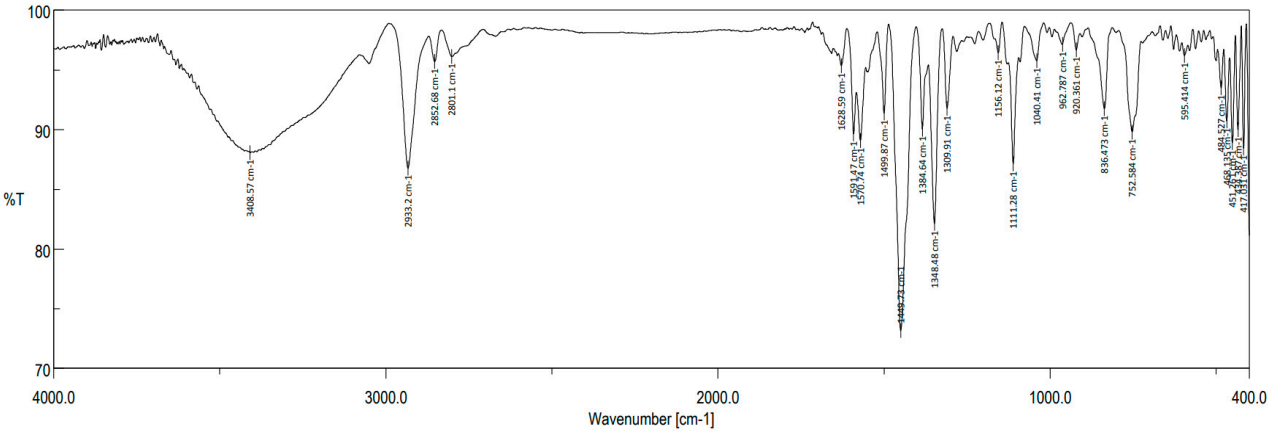


Fig. S2. FTIR spectrum of complex **2** measured in KBr disks.

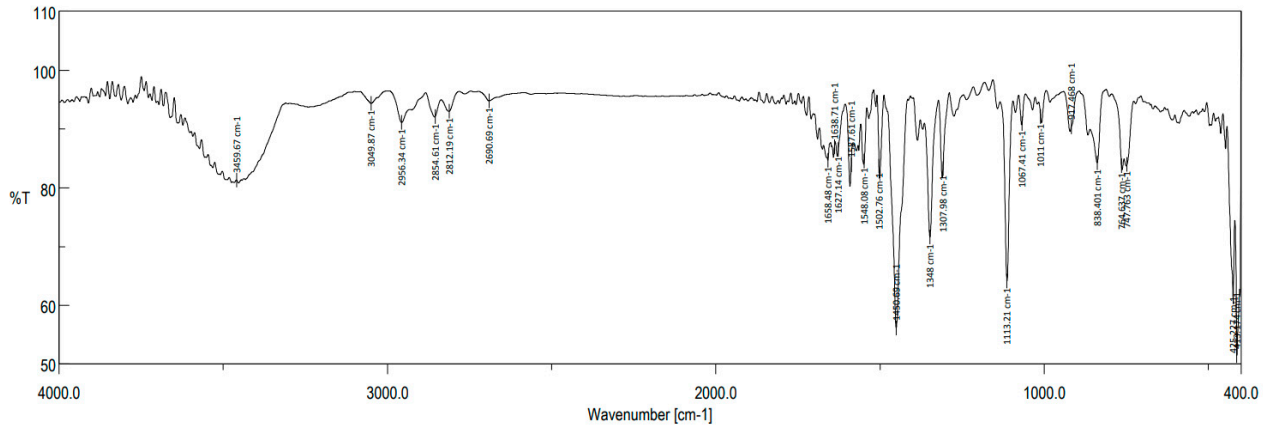


Fig. S3. FTIR spectrum of complex **3** measured in KBr disks.

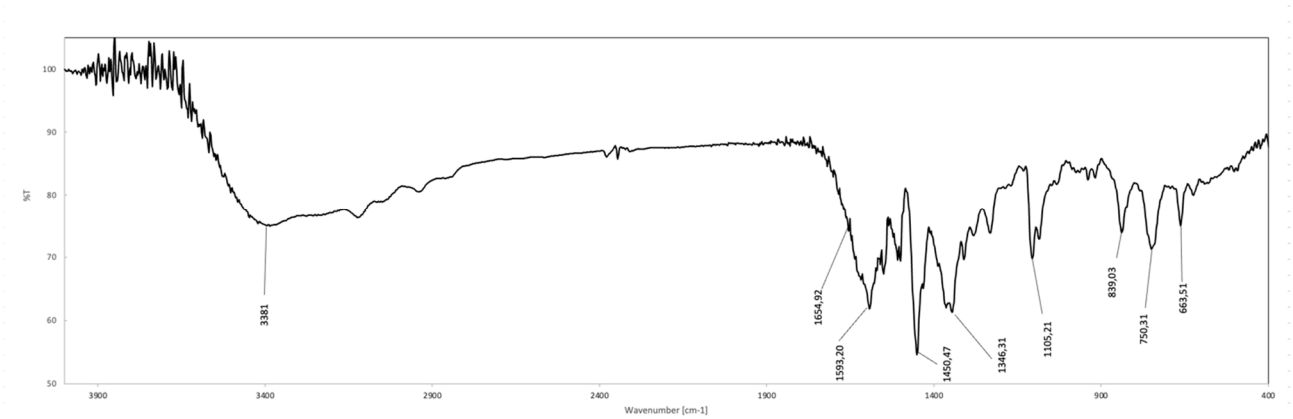


Fig. S4. FTIR spectrum of complex **4** measured in KBr disks.

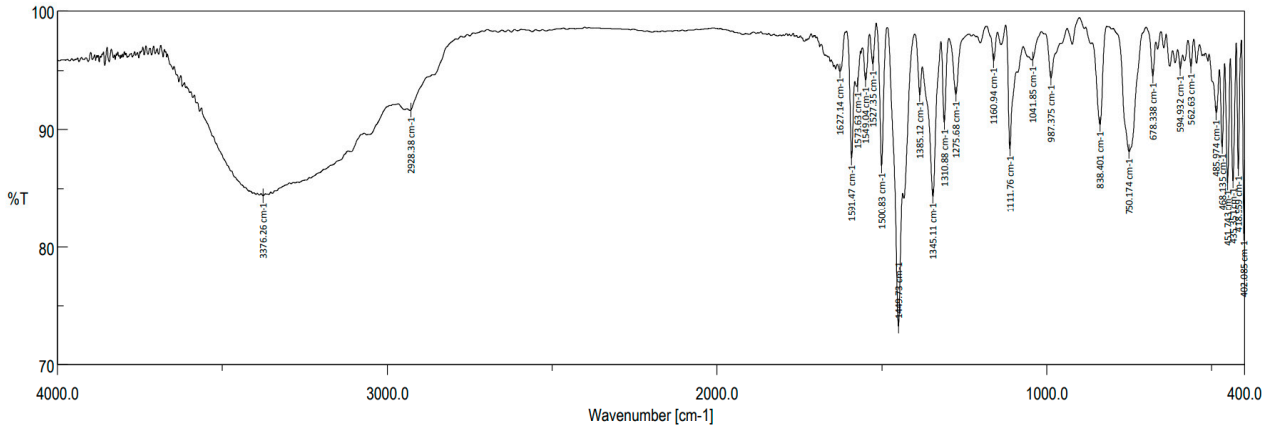


Fig. S5. FTIR spectrum of complex **5** measured in KBr disks.

S2 – ESI-MS data

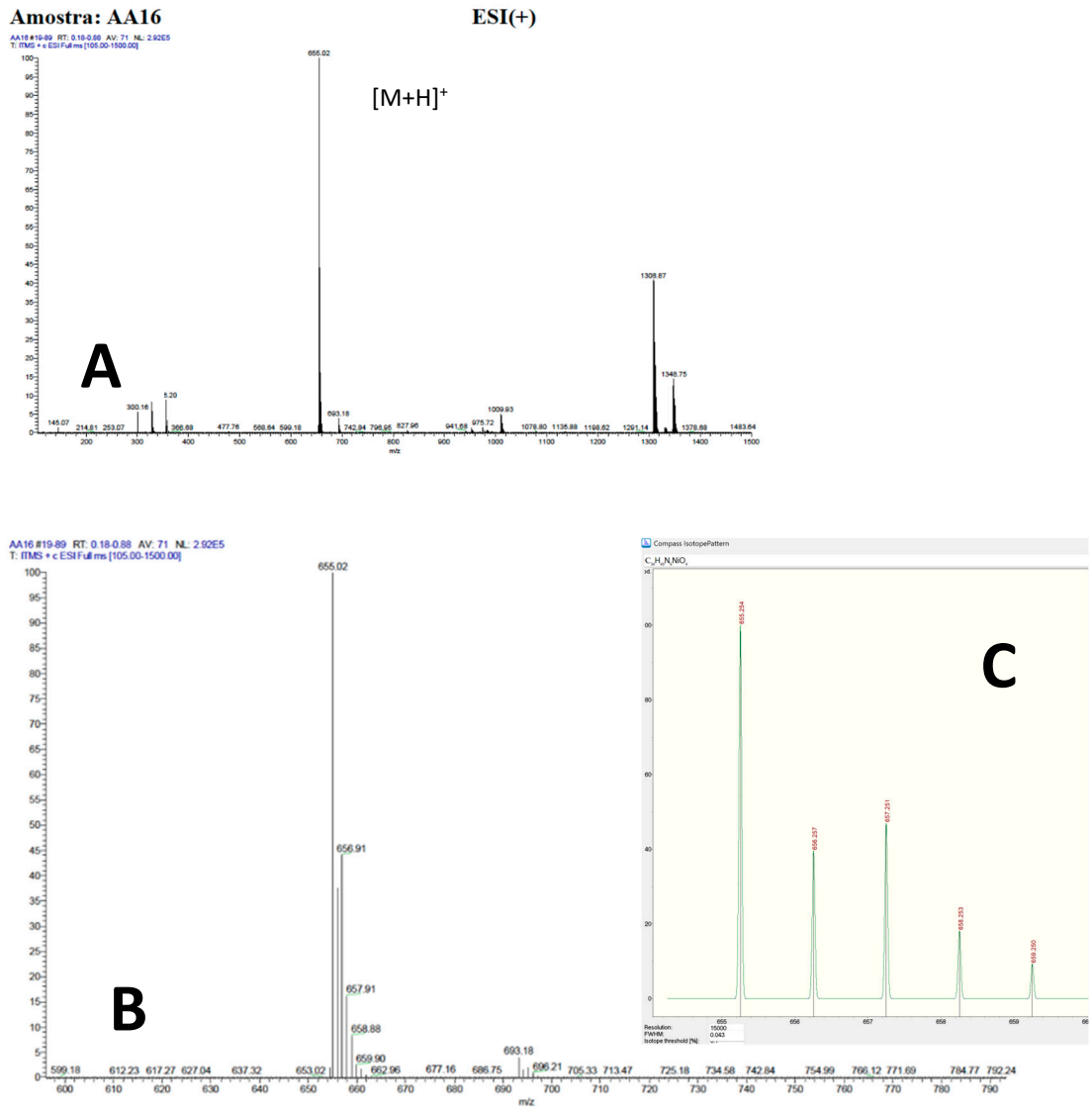


Fig S6. A and B) ESI-MS spectrum of complex **1** in positive mode. C) Expected isotopic pattern for the protonated molecule.

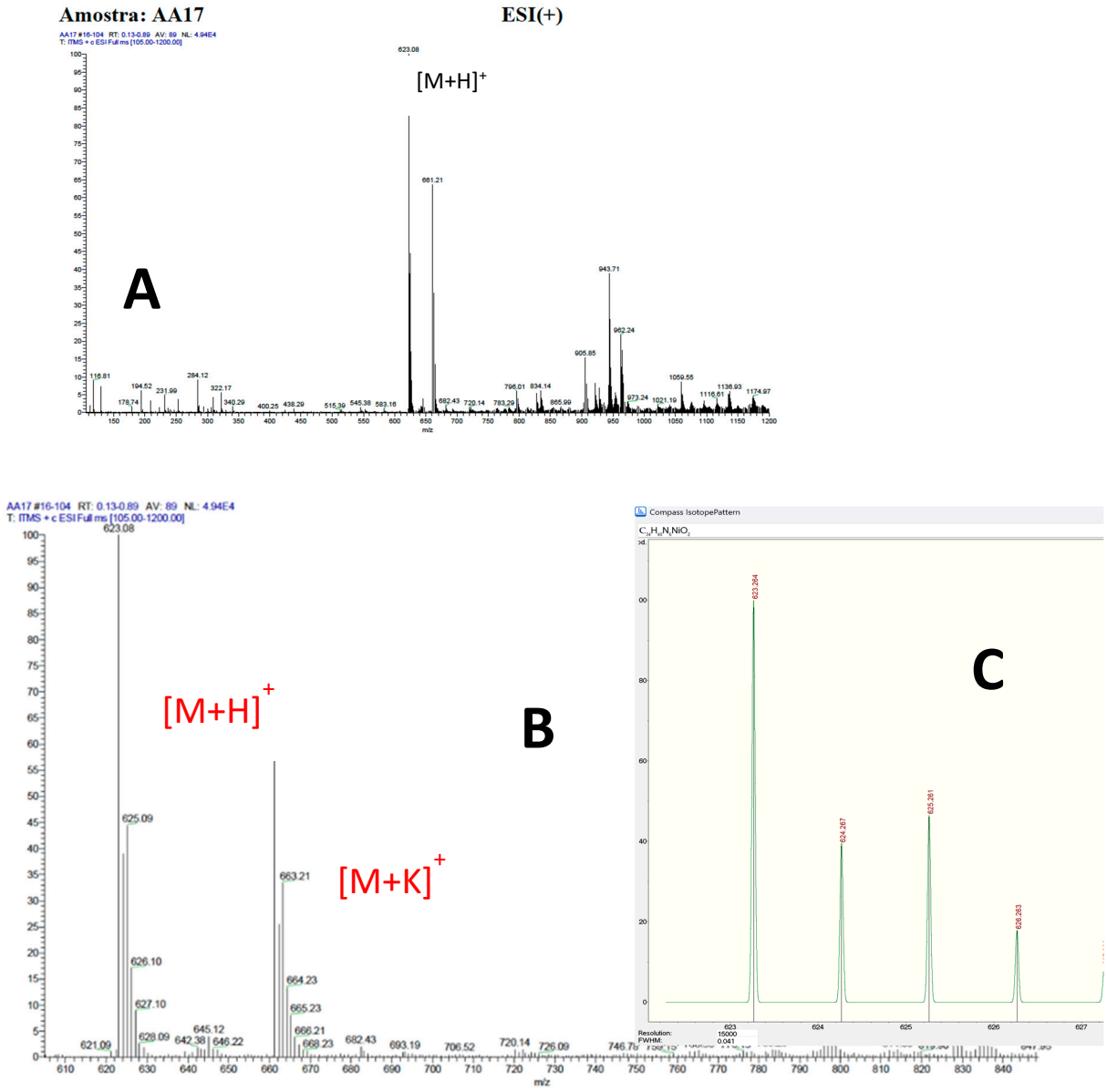


Fig S7. A and B) ESI-MS spectrum of complex **2** in positive mode. C) Expected isotopic pattern for the protonated molecule.

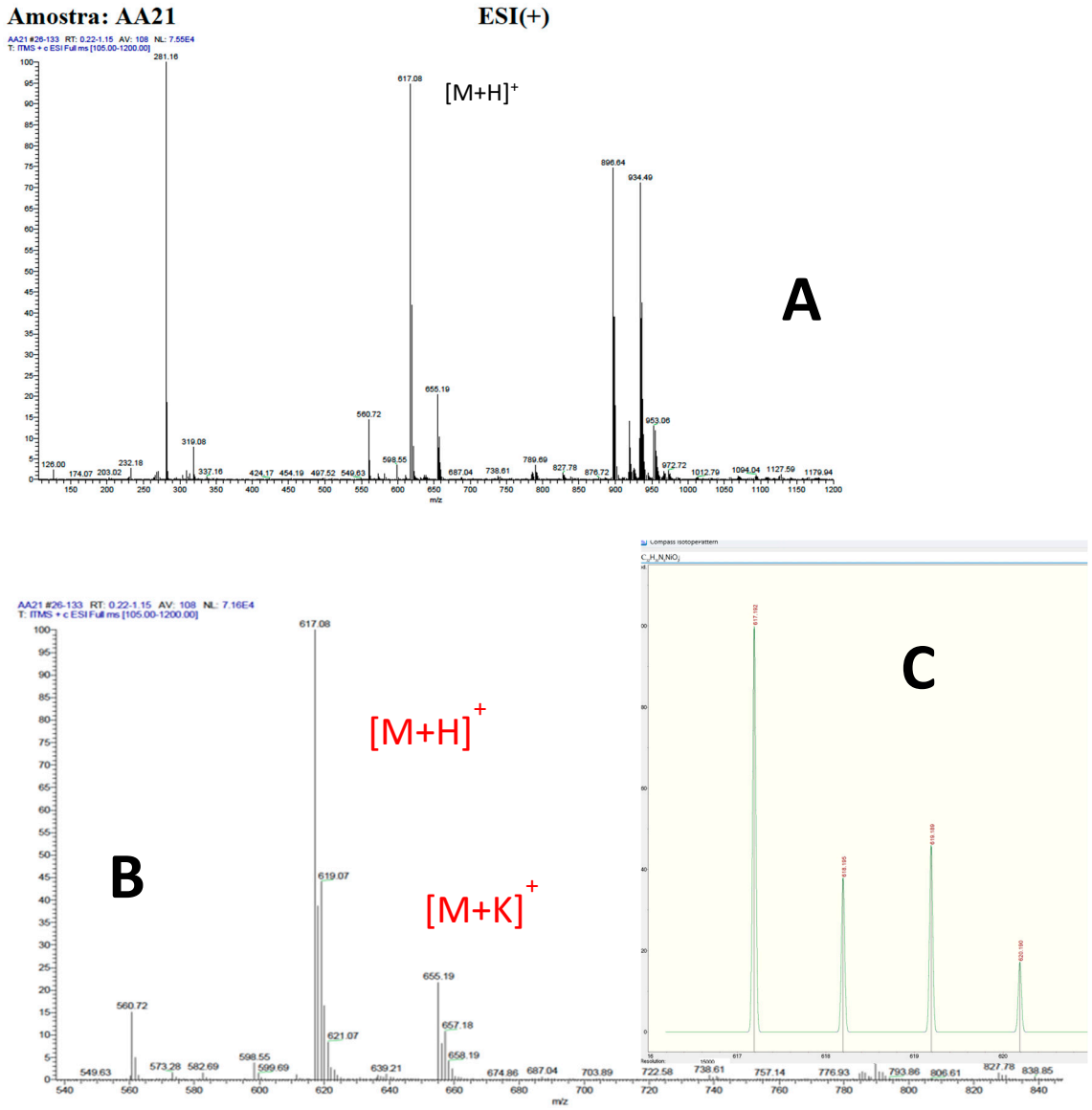


Fig S9. A and B) ESI-MS spectrum of complex **4** in positive mode. C) Expected isotopic pattern for the protonated molecule.

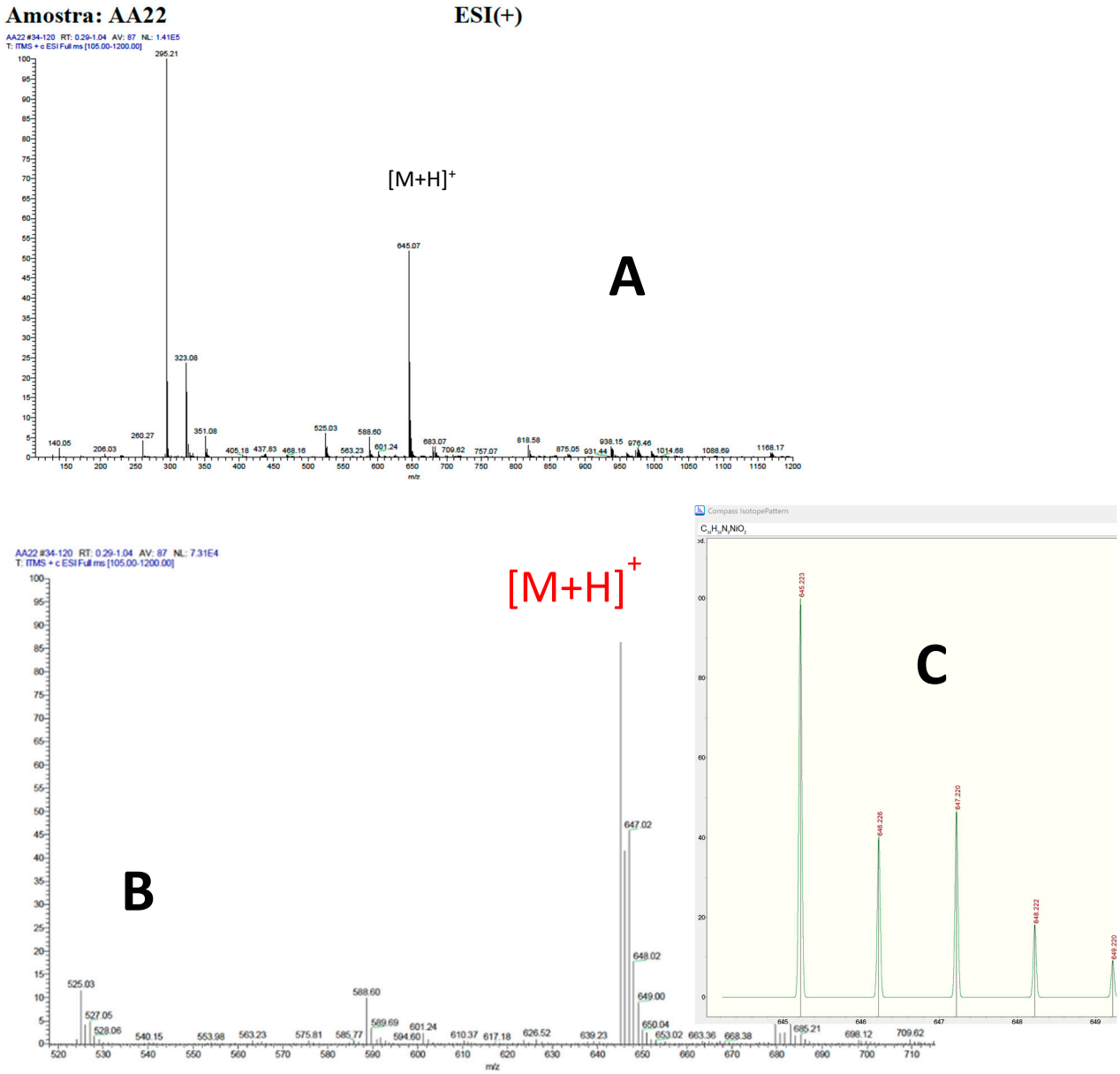


Fig S10. A and B) ESI-MS spectrum of complex **5** in positive mode. C) Expected isotopic pattern for the protonated molecule.

S3 – UV-Vis molecular spectra

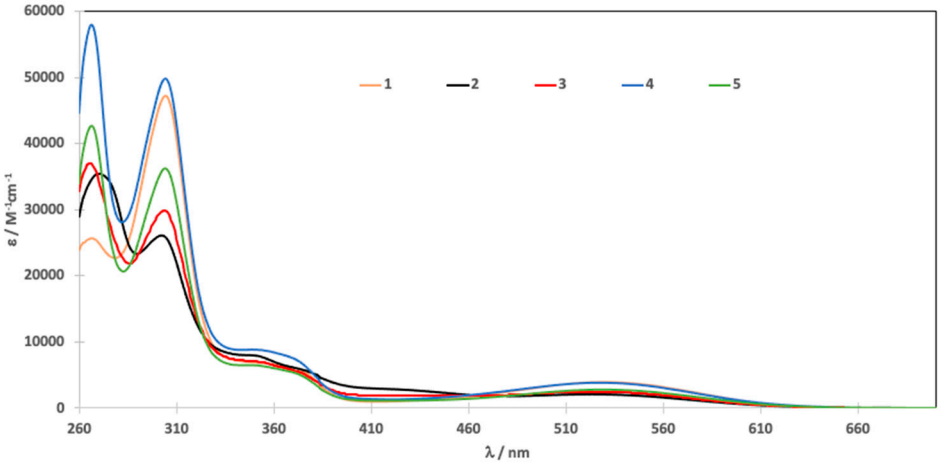


Fig. S11. UV-vis absorption spectra of complexes **1**-**5** measured in DMSO.

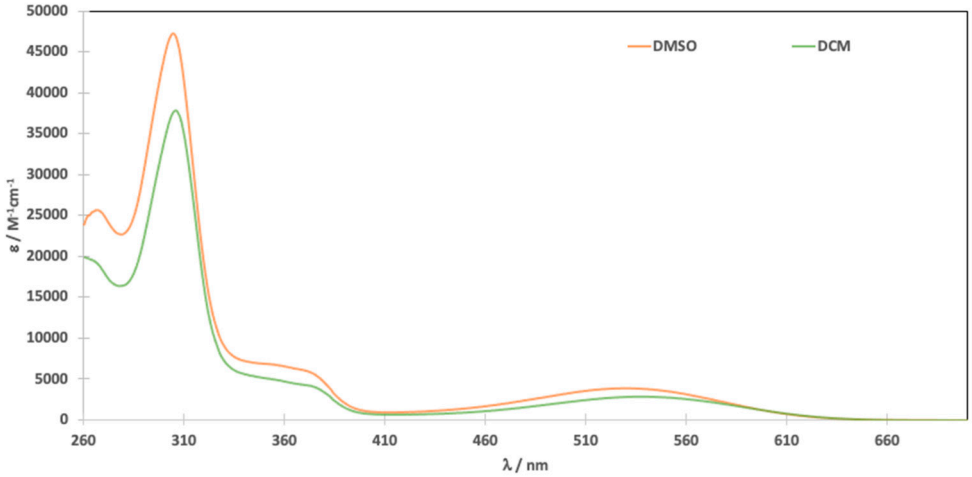


Fig. S12. UV-vis absorption spectra of complex **1** measured in DMSO and CH_2Cl_2.

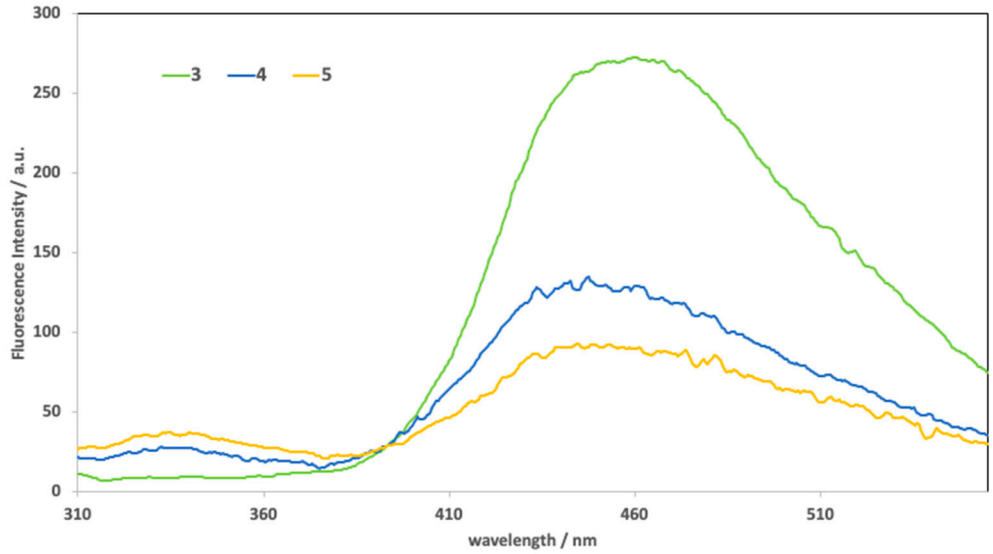


Fig. S13. Fluorescence emission spectra measured for complexes **3** - **5** in DMSO with λ_{ex} = 340 nm.

S4 – SCXRD characterization

Table S1. Selected bond lengths (Å) and angles (°) for complex **1**.

Bond lengths (Å)			
Ni1-N11#1	1.9776(18)	Ni1-N11	1.9777(18)
Ni1-O2	2.1521(16)	Ni1-O2#1	2.1521(16)
Ni1-N14#1	2.1536(19)	Ni1-N14	2.1537(19)
Bond angles (°)			
N11#1-Ni1-N11	178.56(11)	N11#1-Ni1-O2	102.76(7)
N11-Ni1-O2	78.21(7)	N11#1-Ni1-O2#1	78.21(7)
N11-Ni1-O2#1	102.76(7)	O2-Ni1-O2#1	97.19(9)
N11#1-Ni1-N14#1	76.70(7)	N11-Ni1-N14#1	102.33(7)
O2-Ni1-N14#1	87.84(7)	O2#1-Ni1-N14#1	154.91(6)
N11#1-Ni1-N14	102.33(7)	N11-Ni1-N14	76.70(7)
O2-Ni1-N14	154.91(6)	O2#1-Ni1-N14	87.84(7)
N14#1-Ni1-N14	97.99(10)		

Table S2. Selected bond lengths (Å) for **Zn(L3)$_2$** [1] and complex **1** [19].

	Zn(L3)$_2$		**1**
Zn1-N11	2.024(3)	Ni1-N11#1	1.9776(18)
Zn1-O24	2.045(3)	Ni1-O2#1	2.1521(16)
Zn1)-N(14)	2.404(4)	Ni1-N14#1	2.1536(19)
Zn1-N33	2.031(3)	Ni1-N11	1.9777(18)
Zn1-O2	2.096(3)	Ni1-O2	2.1521(16)
Zn1-N36	2.465(5)	Ni1-N14	2.1537(19)

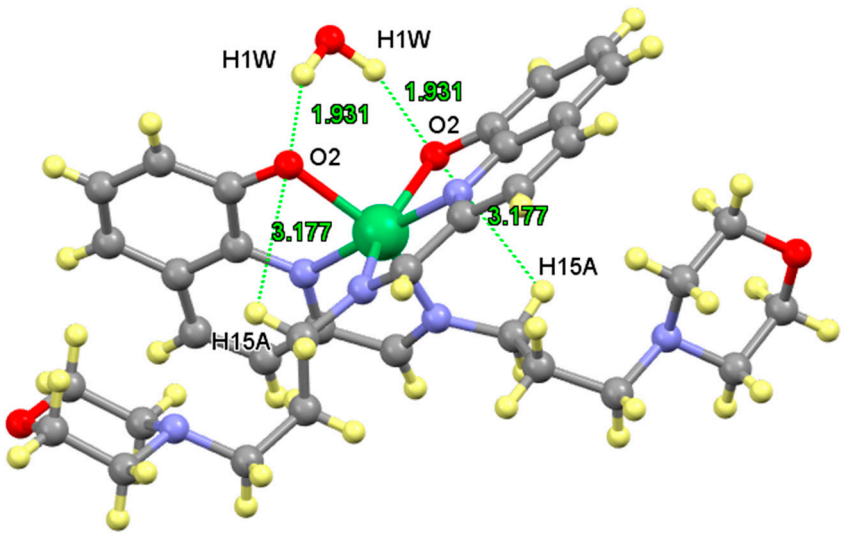
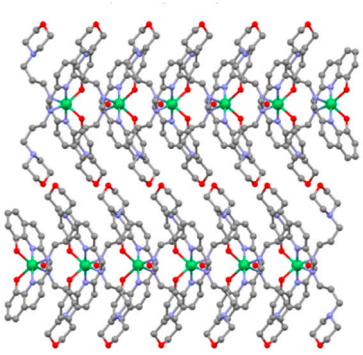
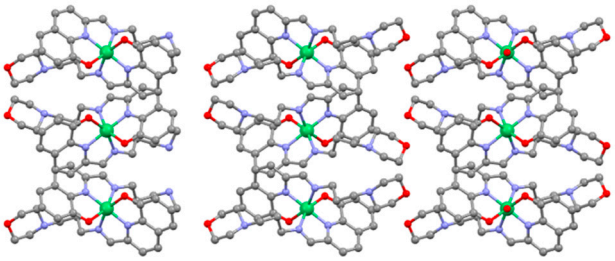


Fig. S14. Intramolecular hydrogen bonds in complex **1**.

A)



B)



C)

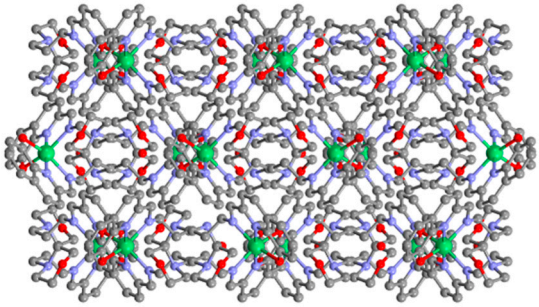


Fig. S15. Packing of complex **1** along the **A)** a axis, **B)** b axis and **C)** c axis.

S5 – Solution stability

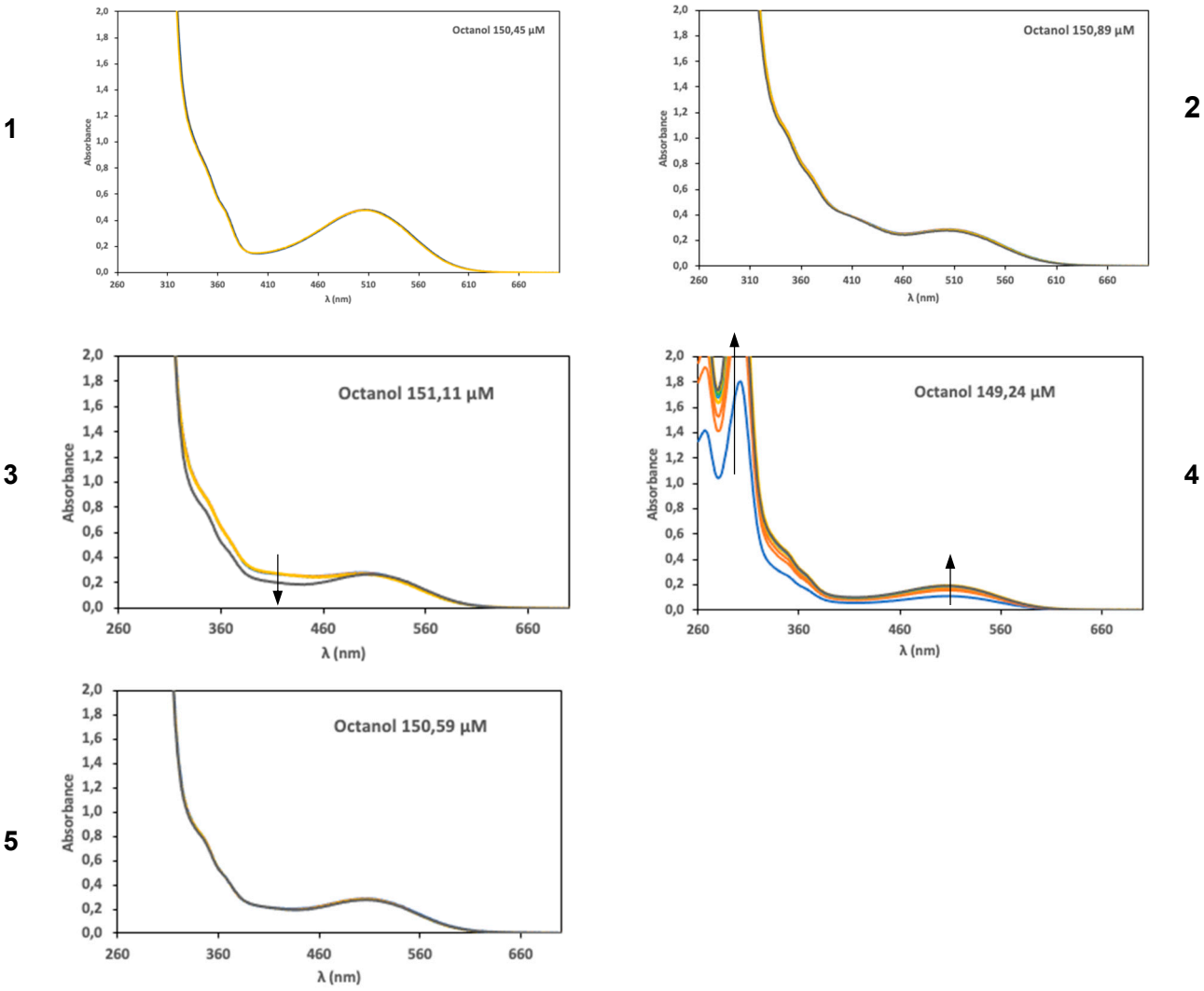
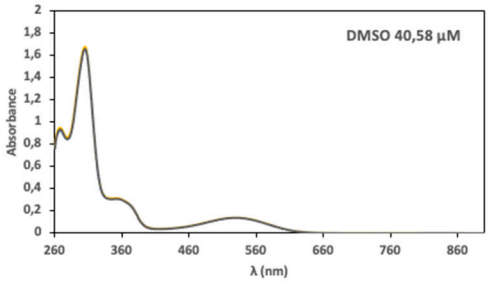
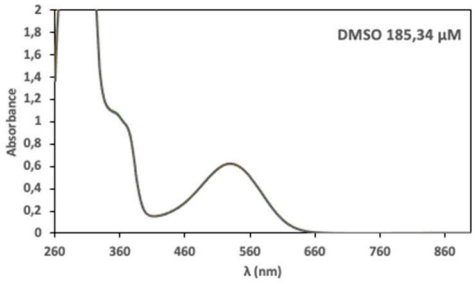


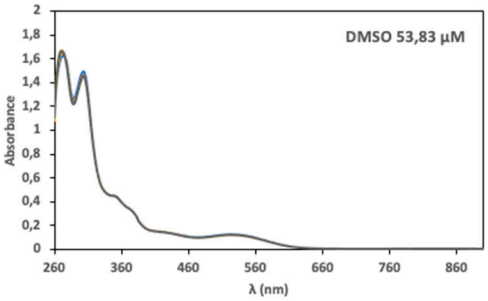
Fig. S16. Stability of the complexes monitored by UV-Vis absorption for 24 h (concentrations indicated in the figures) in *n*-octanol.

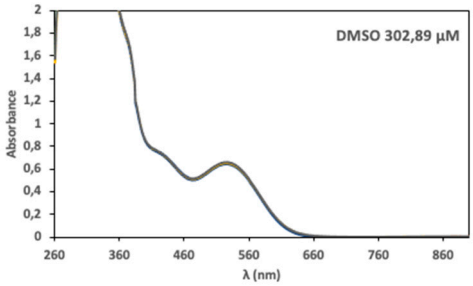
1


DMSO 40,58 µM
Absorbance
λ (nm)

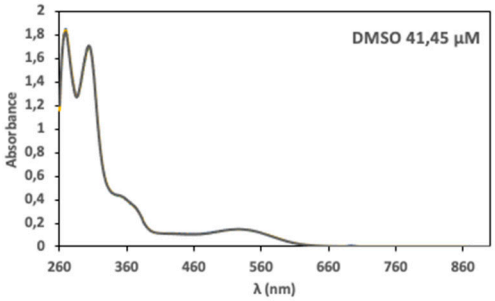

DMSO 185,34 µM
Absorbance
λ (nm)

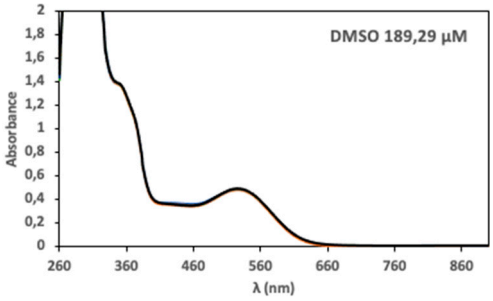
2


DMSO 53,83 µM
Absorbance
λ (nm)

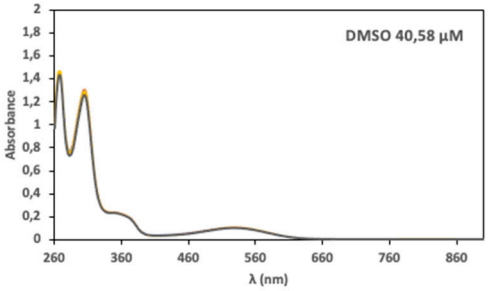

DMSO 302,89 µM
Absorbance
λ (nm)

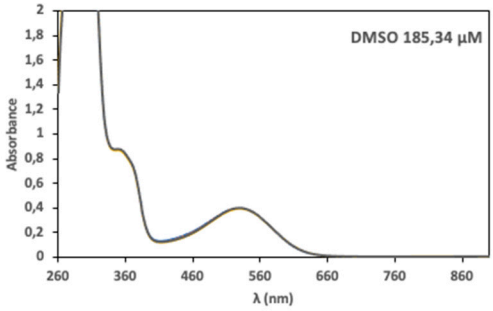
3


DMSO 41,45 µM
Absorbance
λ (nm)


DMSO 189,29 µM
Absorbance
λ (nm)

4


DMSO 40,58 µM
Absorbance
λ (nm)


DMSO 185,34 µM
Absorbance
λ (nm)

5

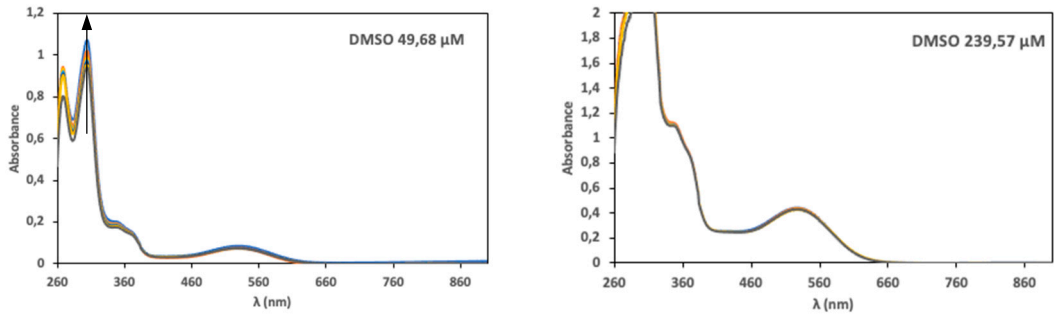
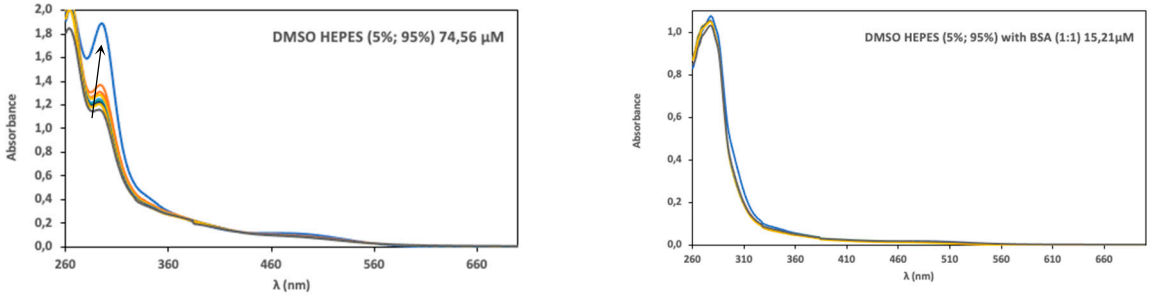
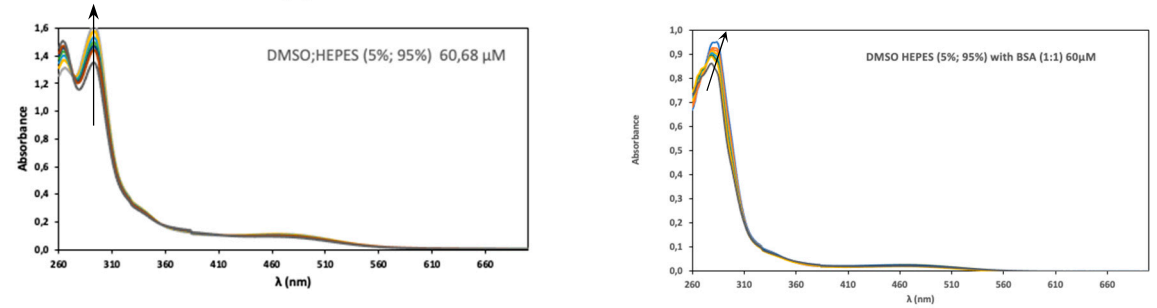


Fig. S17. Stability of the complexes monitored by UV-Vis absorption for 24 h at two concentrations (indicated in the figures) in DMSO.

2



4



5

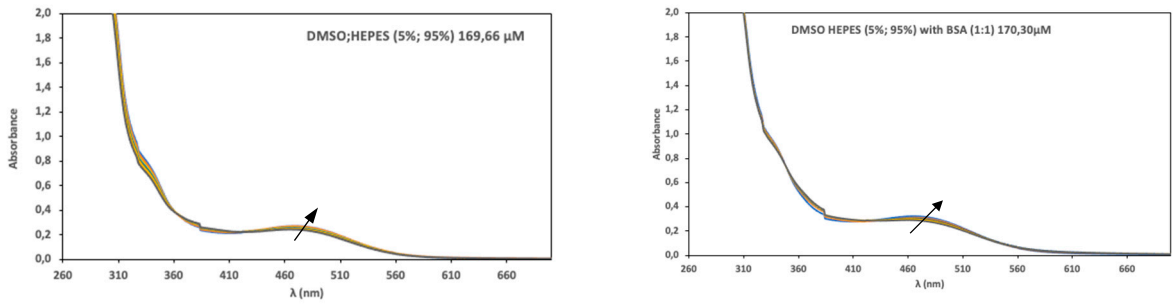


Fig. S18. Stability of complexes **2**, **4** and **5**, monitored by UV-Vis absorption for 24 h (concentrations indicated in the figures) in DMSO:HEPES (10 mM, pH 7.4) (5%:95%) in the absence and in the presence of BSA in 1:1 molar ratio.

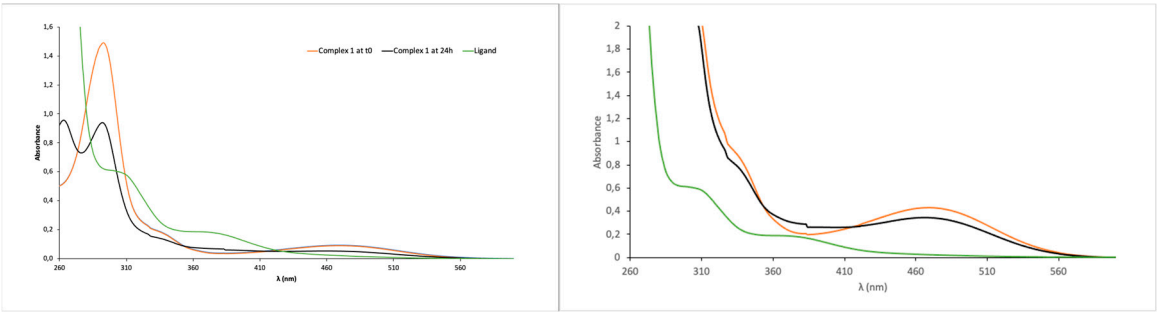


Fig. S19. Stability of complex **1** monitored by UV-Vis absorption after dissolution and after 24 h and the free ligand in DMSO:HEPES (10 mM, pH 7.4) (5%:95%). Concentrations: A) [**1**]= 38 µM and [L]=227 µM. B) [**1**]= 38 µM and [L]=227 µM.

S6 – BSA binding

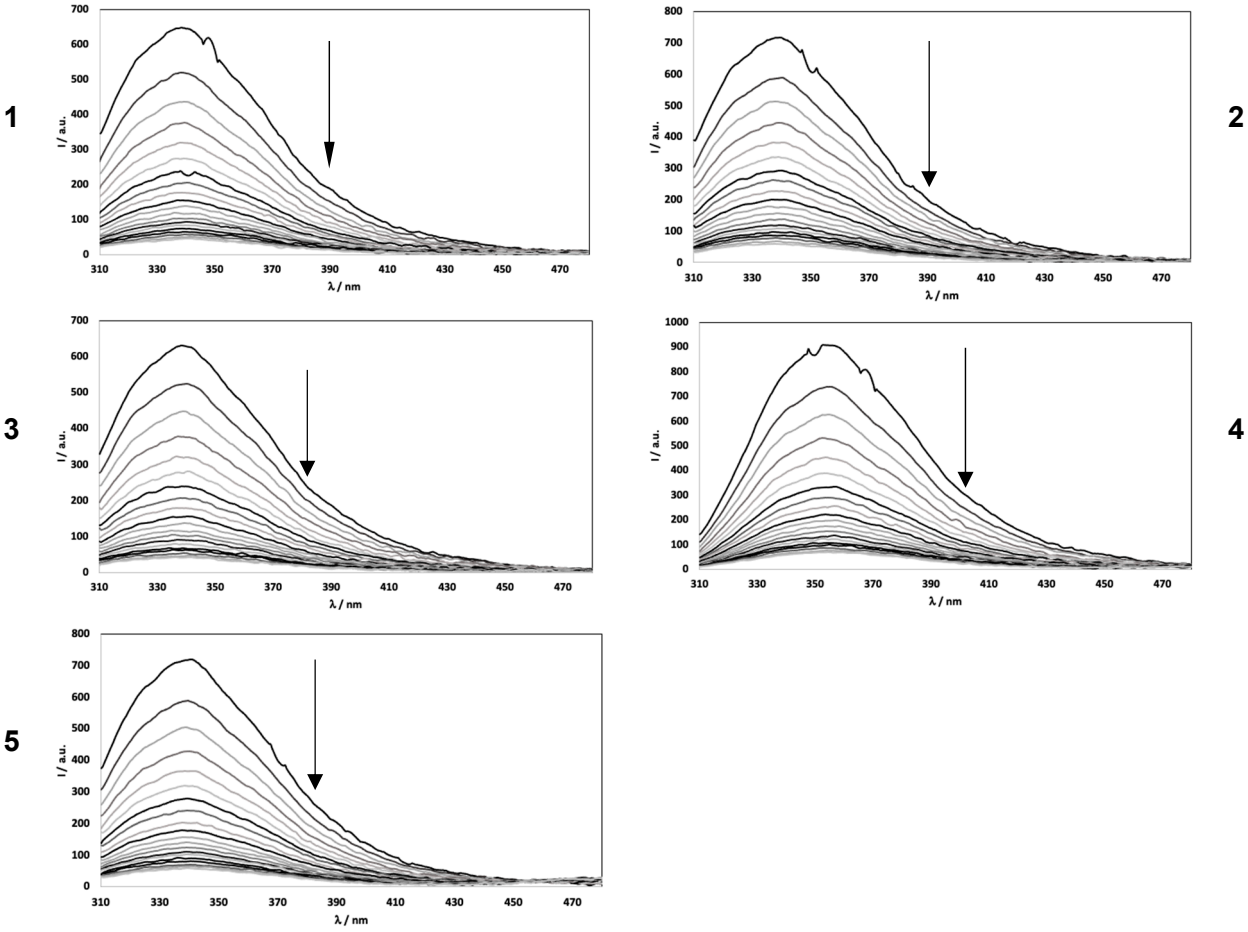


Fig. S20. Fluorescence emission spectra measured for the quenching of BSA (~2-3 μM) with complexes **1** - **5** (λ_{exc} = 295 nm, %DMSO <1.5 (v/v). Arrows indicate spectral evolution with increasing complex concentrations (between 0 and 25 μM).